ISTITUTO NAZIONALE DI FISICA NUCLEARE

LABORATORI NAZIONALI DI FRASCATI

INFN-14-16/LNF
25th Novembre 2014

Hybrid Scheme of Positron Source At SPARC_Lab LNF Facility: Channeling Radiation and Amorphous Photon Converter

S.V. Abdrashitov[1,2], O.V. Bogdanov[1], S.B. Dabagov[3,4], Yu.L.Pivovarov[1], T.A.Tukhfatullin[1]

[1)]National Research Tomsk Polytechnic University, Lenin Ave 30, 634050 Tomsk, Russia
[2)]National Research Tomsk State University, Lenin Ave 36, 634050 Tomsk, Russia
[3)]INFN-Laboratori Nazionali di Frascati Via E. Fermi 40, I-00044 Frascati, Italy
[4)]RAS PN Lebedev Physical Institute & NRNU MEPhI, Moscow, Russia

Abstract

The hybrid scheme of the positron source for SPARC_LAB LNF facility (Frascati, Italy) is proposed. The comparison of the positron yield in a thin amorphous W converter of 0.1 mm thickness produced by bremsstrahlung, by axial <100> and planar (110) channeling radiations in a W crystal is performed for the positron energy range of $1 \div 3$ MeV. It is shown that channeling radiation by 200 MeV electrons (parameters of SPARC LNF Frascati) in a 10 μm W crystal can produce positrons in the radiator of 0.1 mm thickness with the rate of $10–10^2$ s^{-1} at planar channeling and of $10^3–10^4$ s^{-1} at axial channeling.

Published by ***SIDS–Pubblicazioni***
Laboratori Nazionali di Frascati

PACS.: 78.70.-g, 61.85.+p, 61.80.Fe, 41.75.Fr, 41.75.Ht

1 POSITRON BEAM SOURCES

The problem of positron beam generation remains of interest during last decade, in connection with the physics of slow positrons and positronium atom beams [1–4] and with searching for effective positron source for electron–positron colliders [5–8]. Several schemes are suggested for intense positron beam generation, and all of them are based on the initial intense photon beam generated in different ways: bremsstrahlung (B) [9], channeling radiation (CR) [5-6, 10-11] or coherent bremsstrahlung (CB) [7-9], Compton scattering [11], and even undulator radiation [12]. In general, we can define the following schemes for positron production (see in Table 1):

1. The one-component scheme with amorphous target. B from the primary intense electron beam of several GeV is used for the photoproduction of e^--e^+ pair in the same target.
2. The one-component scheme with crystal target is similar to Scheme No 1, however, the yield of positrons is higher due to coherent effects in crystalline target.
3. In the two-component (hybrid) scheme electron beam incident to crystalline target (radiator) for CR or CB production. Emitted photon beam is separated from charged particles and incident to amorphous target (convertor) for conversion into e^--e^+ pairs.
4. In another two-component scheme photons from laser beam due to inverse Compton scattering on multi-GeV electrons obtain enough energy to produce e^--e^+ pairs and then photons are sent to converter.
5. The scheme suggested for ILC - the so-called undulator-based positron source.

Table 1: Review of the basic schemes of the positron sources

Scheme	Description	e^- energy GeV	Yield e^+/e^-	Ref.
1	amorphous W, 8 mm	10	~0.02	[9]
1	amorphous W, 4 mm	10	~0.005	[9]
1	amorphous W, 1.2 mm	1.2	~0.0002	[5]
1	amorphous W, ~0.35 r.l.	1.2	~0.0364	[7]
1	amorphous Si, ~0.35 r.l.	1.2	0.0534	[7]
2	<111> W, 8 mm	10	~0.04	[9]
2	<111> W, 4 mm	10	~0.015	[9]
2	<100> W, 1.2 mm	1.2	~0.0005	[5]
2	<100> W, ~0.35 r.l.	1.2	~0.102	[7]
2	<100> Si, ~0.35 r.l.	1.2	0.0331	[7]
3	radiator – <111> W, ~0.5 r.l. converter – amorphous W, ~ 2.0 r.l.	2 ÷ 6	0.02 ÷ 0.03	[8]
3	radiator – <111> W, 1, 2 and 4 mm converter – amorphous W, 1 ÷ 10 mm	10	2 ÷ 14 (1mm) 3 ÷ 16 (2mm) 3 ÷ 13 (4mm)	[11]
4	radiator – inverse Compton scattering converter – amorphous W	3 ÷ 5	~ 1	[11]
5	radiator – undulator (period 2.54 mm, K=0.17) converter – amorphous W, ~ 0.2 r.l.	46.6	$\sim 10^{-5}$	[12]

Table 1 presents the main parameters of the several schemes of positron sources including yield of positrons and basic characteristics (primary electron beam energy, radiator and converter materials, the thickness of targets in radiation length – r.l.).

The energy spectrum of CR from relativistic electrons in a crystal is characterized by a bright maximum, position of which depends on the energy of the initial electron beam and on the crystal both alignment and type.

The principal difference between Schemes No.1 and No.3 is obvious: the B spectrum is much broader than the CR one. This means, the positron energy spectrum will be broader in the case of B.

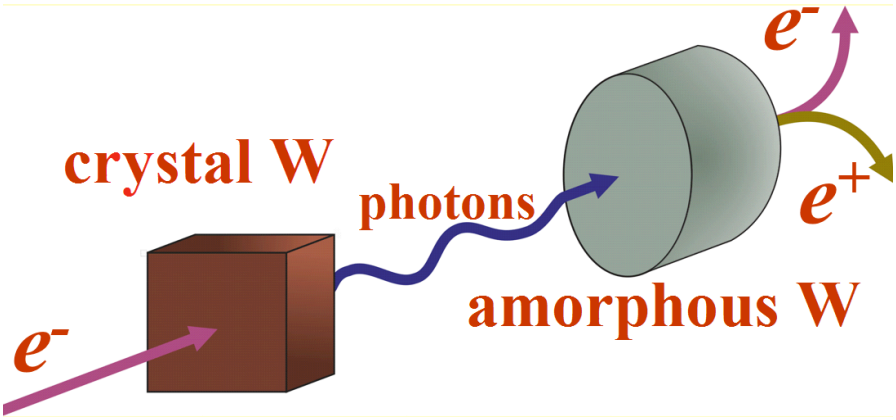

Figure 1: The scheme of hybrid positron source using CR from primary electron beam.

In this work we analyze the hybrid Scheme No.3 (Fig. 1) aiming at the determination of the energy spectrum of emitted positrons and at the estimation of a positron yield. Photon source is CR from 200, 800 and 1600 MeV electrons at (110) and <100> channeling in W crystal (200 MeV is the foreseen electron energy at SPARC_LAB). For radiation of 200 MeV electrons the contribution of B is taken into account. The thickness of a W crystal (radiator) is 10 μm that less than the dechanneling length [13]. Here, we restrict our consideration by choosing a thin W convertor to neglect multiple scattering and energy loss. Knowing the positrons energy spectrum created by CR in a thin convertor, it becomes easy to apply known results for simulating the scheme with a thick photon-pair convertor.

2 SIMULATION OF ELECTRON CR SPECTRA IN W CRYSTAL

General properties of CR are well described in [14-15]. The calculations of CR spectra in the frame of binary collision model was carried out in [16]. The BCM-1.0 code [17] developed by the authors enables to calculate the real trajectories and CR spectra of both planar and axial channeled electrons in crystals. Recently, this code was used to calculate the orientation dependence of the CR total yield [18].

Figures 2 present the intensity spectra (energy radiated during penetration through a crystal per unit of the crystal length) of radiation from 200 MeV electrons at planar (Fig. 2a) and axial (Fig. 2b) channeling in W. For the SPARC primary 200 MeV electron beam the brilliant peak of radiation at planar channeling is located near 1÷2 MeV, thus allowing creation of positrons with maximal kinetic energy about 1 MeV. The spectrum of CR form axially channeled 200 MeV electrons is much broader, and, moreover, it extends up to 20 MeV with the maximum at 5 MeV, thus resulting in a positron yield with maximal kinetic

energy about 4 MeV. In order to get maximal total yield of CR the axial channeling in radiator results to be a better choice, however, the planar case has been studied as well.

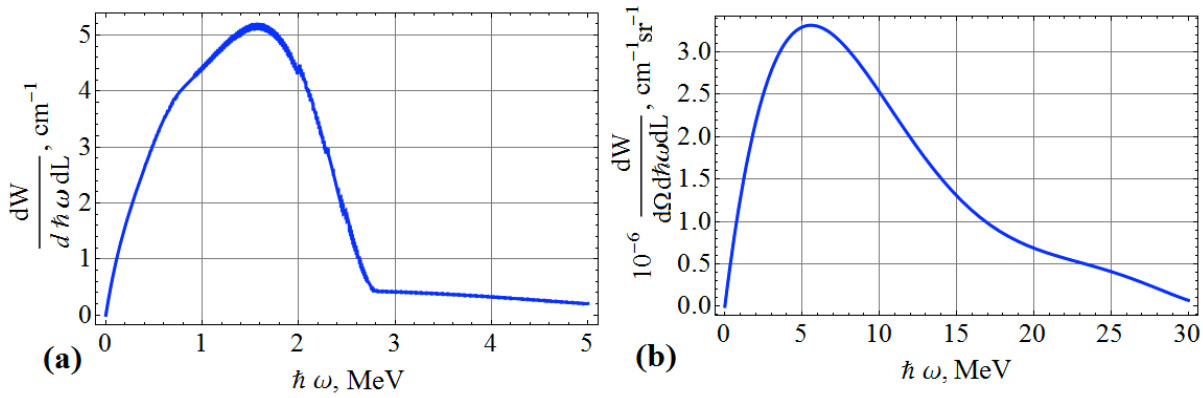

Figure 2: (a) CR intensity spectra from 200 MeV electrons (SPARC energy) at (110) planar channeling in W crystal; (b) Spectral-angular distribution of CR from 200 MeV electrons at <100> axial channeling in W (forward direction, θ_γ=0).

The simulation of the radiation from 200 MeV electrons in (110) W shows that the planar (110) CR intensity (Fig. 2a) and the bremsstrahlung intensity (Fig. 3) are comparable in values within the range of photon energies 1÷3 MeV. Thus, for the correct calculation of the yield of positrons in the range of energy up to 2 MeV one need to take into account the contributions of both types of radiation. For the comparison of the axial CR intensity (Fig. 2b) and the bremsstrahlung intensity (Fig. 3) we involve total yield of radiation [18]. The total yield of bremsstrahlung is twice larger than the total yield of axial CR, but the axial CR spectrum is almost 20 times narrower than bremsstrahlung one, so the maximum of axial CR spectrum is expected to be 10 times larger than the maximum for bremsstrahlung spectrum. Accurate calculations are carried out later.

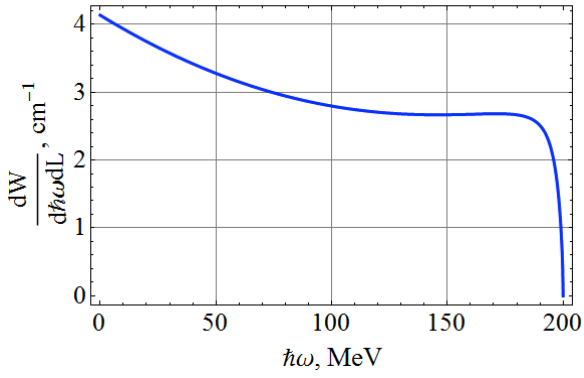

Figure 3: Bremsstrahlung intensity spectrum from 200 MeV electrons in amorphous W calculated according Schiff formulae [19].

3 ELECTRON-POSITRON PAIR PHOTOPRODUCTION PER ONE W ATOM

Most commonly, for the calculation of the e^--e^+ pair production by photon in atomic field the Bethe-Heitler formula taking into account various effects is used [20-22]:

$$\frac{d\sigma}{dE_P} = \frac{\alpha r_e^2 Z[Z+\xi(Z)]}{E_\gamma} \cdot \left\{ \begin{array}{l} [(\frac{E_P}{E_\gamma})^2 + (1-\frac{E_P}{E_\gamma})^2][\Phi_1(\delta) - F(Z)] + \\ \frac{2}{3}\frac{E_P}{E_\gamma}(1-\frac{E_P}{E_\gamma})[\Phi_2(\delta) - F(Z)] \end{array} \right\}, \qquad (1)$$

where α is the fine-structure constant and r_e is the classical electron radius, Z is the atomic number. Here E_γ is the energy of the photon and E_p is the total energy of positron. As the minimal energy of electron or positron is equal to it's rest mass, the bound for E_p are therefore: $m_e c^2 \leq E_p \leq E_\gamma - m_e c^2$. The screening parameter δ is a function of E_p and E_γ:

$$\delta = \frac{136}{Z^{1/3}} \frac{m_e c^2 E_\gamma}{E_P(E_\gamma - E_P)}.$$

Two screening functions, the same as in the B case [21], are introduced in the Bethe-Heitler formula:

for $\delta \leq 1$: $\Phi_1(\delta) = 20.867 - 3.242\delta + 0.625\delta^2$,

$\Phi_2(\delta) = 20.209 - 1.930\delta - 0.086\delta^2$;

for $\delta > 1$: $\Phi_1(\delta) = \Phi_2(\delta) = 21.12 - 4.184\ln(\delta + 0.952)$.

The electron cloud gives an additional contribution to the pair creation:

$$\xi(Z) = \frac{\ln(1440/Z^{2/3})}{\ln(183/Z^{1/3}) - f_c(Z)}.$$

The Coulomb correction function:

for $E_\gamma < 50 MeV$: $F(Z) = 4/3\ln(Z)$;

for $E_\gamma \geq 50 MeV$: $F(Z) = 4/3\ln(Z) + 4 f_c(Z)$,

where $f_c(Z) = (\alpha Z)^2 \left[\frac{1}{1+(\alpha Z)^2} + 0.20206(\alpha Z)^2 + 0.0083(\alpha Z)^4 - 0.0020(\alpha Z)^6 \right]$.

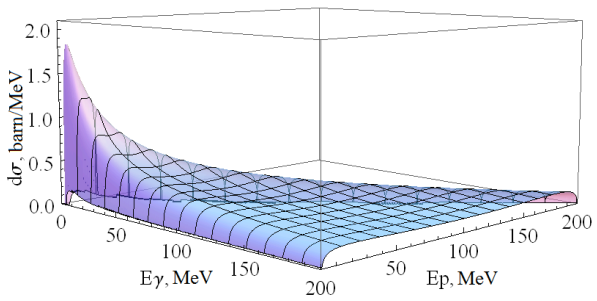

Figure 4: Cross-section of photon conversion (1) into e^--e^+ pair per one W atom as a function of the incident photon and outgoing positron energies.

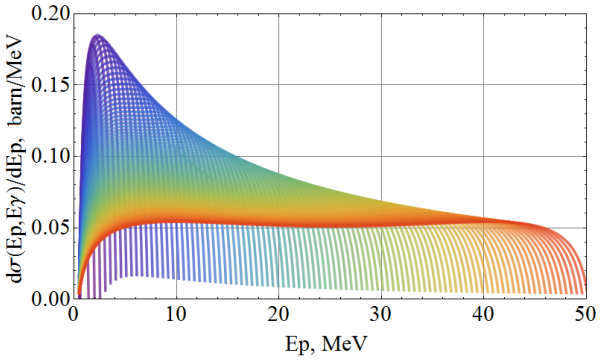

Figure 5: Cross-section of photon conversion (1) into e^--e^+ pair per one W atom as a function of the outgoing positron energy. Lines colors change from violet to red as the energy of photon changes from 1 up to 50 MeV.

The cross-section for the conversion of the photon into e^--e^+ pair per W atom given by equation (1) determines two-dimensional surface (Fig. 4). The presentation of the cross-section for photon conversion into e^--e^+ pair (1) is given by the sections of this surface (Fig. 5), which shows the cross-section of e^--e^+ pair production by the photon of a certain energy [e.g. 13, 20].

An integration of the cross-section of the photon conversion into e^--e^+ pair per one atom (1) over the positron energy E_P:

$$\sigma_{tot}(Z,E_\gamma)=\int\frac{d\sigma(Z,E_P,E_\gamma)}{dE_P}dE_P\,, \qquad (2)$$

gives us the total cross-section of e^--e^+ pair production by the photon of energy E_γ per one atom (Fig. 6). According to Fig. 6, the increase of incident photon energy results in the positron yield growth, but according to Fig. 4 this leads to spreading the positron energy spectrum.

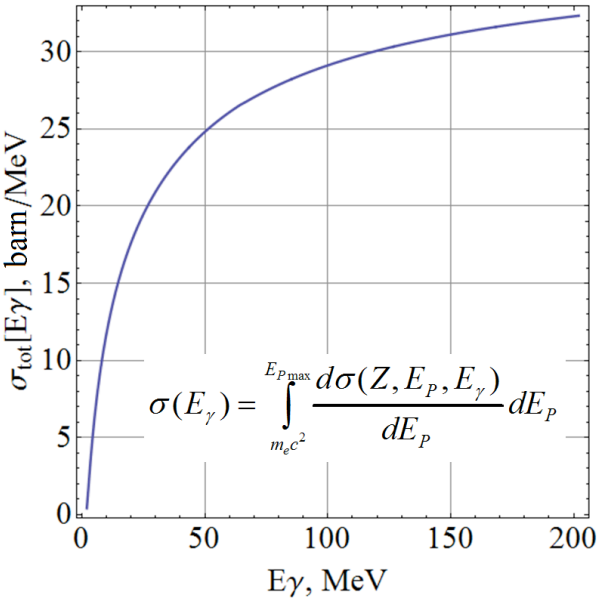

Figure 6: Total cross-section of e^--e^+ pair production per one W atom as a function of the photon of energy E_γ.

4 ELECTRON-POSITRON PAIR PRODUCTION BY CR

The number of photons emitted by the electrons at channeling in the radiator of thickness L = 10 μm can be determined in the following way:

$$N(E_\gamma) = \frac{1}{\hbar\omega}\frac{dW}{d\hbar\omega dL}\cdot L \ (\text{MeV}^{-1}). \qquad (3)$$

The cross-section of e^--e^+ pair production by CR (Fig. 7):

$$\frac{d\sigma_{CH}(Z,E_P,E_\gamma)}{dE_P} = N(E_\gamma)\cdot\frac{d\sigma(Z,E_P,E_\gamma)}{dE_P} \ (\text{barn/MeV}^2). \qquad (4)$$

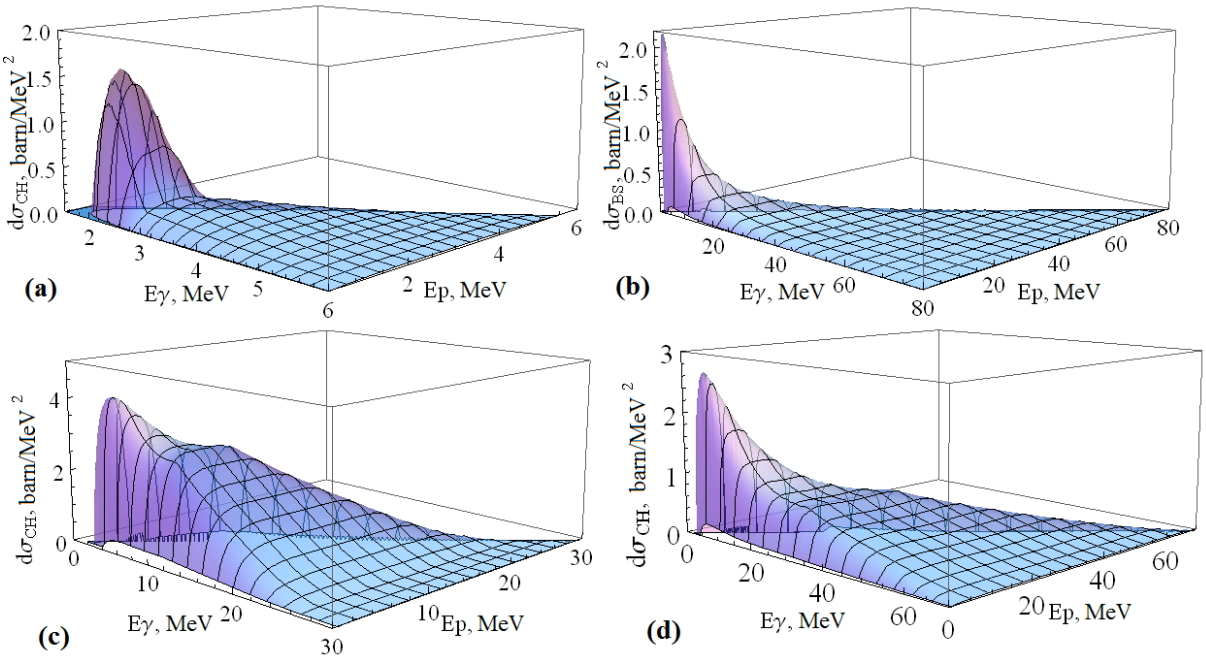

Figure 7: Cross-section of e^--e^+ pair production $N(E_\gamma)\cdot d\sigma(Z,E_P,E_\gamma)/dE_P$ (4) by radiation from: (110) channeled electrons in W: (a) 200 MeV, (c) 800 MeV, (d) 1600 MeV; (b) B from 200 MeV electrons in W.

Thus integral:

$$\sigma(Z,E_P) = \int\frac{d\sigma_{CH}(Z,E_P,E_\gamma)}{dE_P}dE_\gamma \ (\text{barn/MeV}) \qquad (5)$$

determines the spectrum of positrons generated by CR from electrons (Fig. 8).

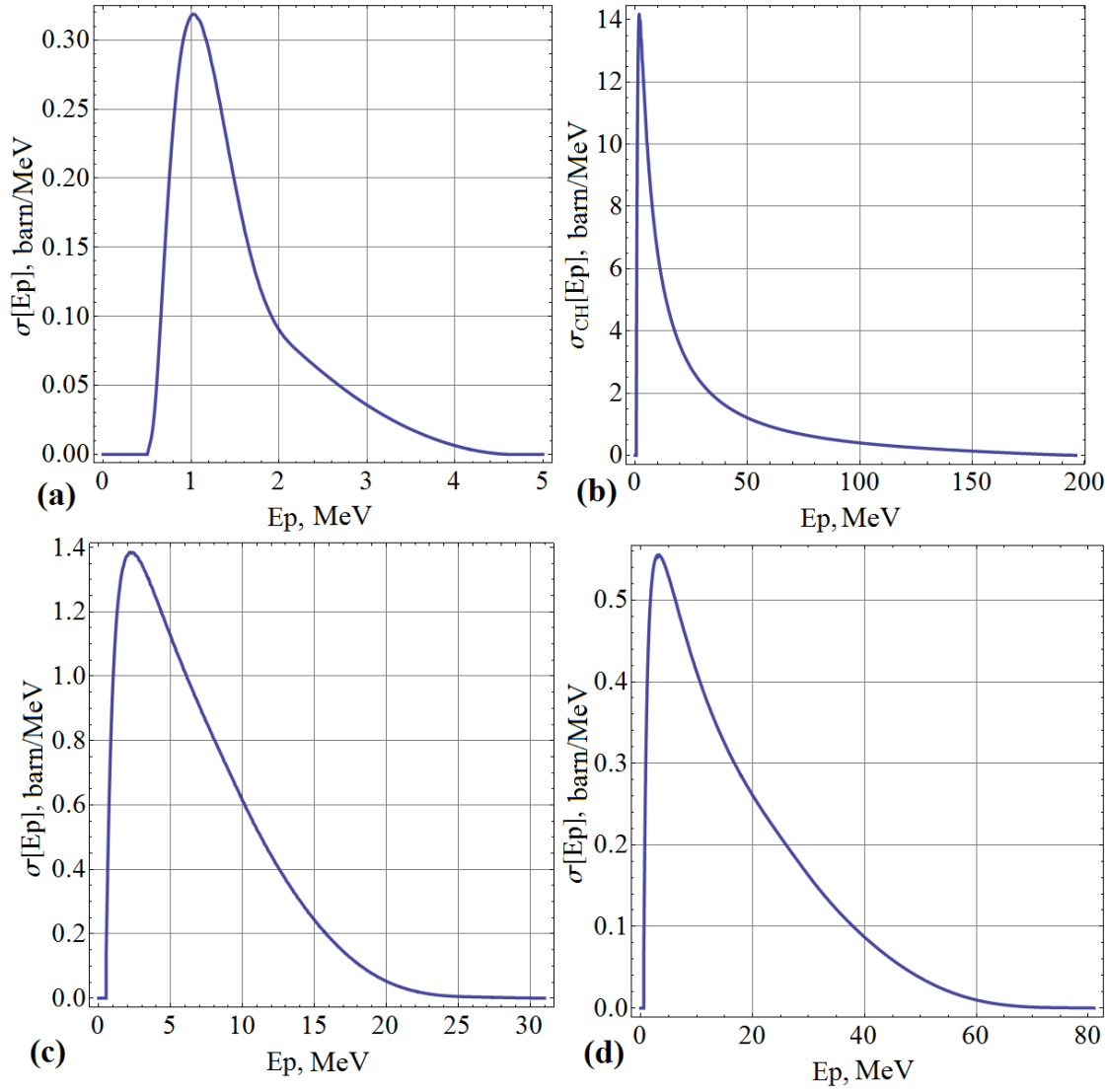

Figure 8: The energy spectra of positrons (6), produced by: (110) CR from electrons W: (a) 200 MeV, (c) 800 MeV, (d) 1600 MeV; (b) B from 200 MeV electrons in W

In the frame of considered Scheme No.3 the yield of positrons from conversion of CR into e^--e^+ pair per one atom determines by the expressions:

for planar channeling $$Y_P = n \cdot L_C \cdot \iint \frac{d\sigma_{CH}(Z, E_P, E_\gamma)}{dE_P} dE_\gamma dE_P \, ; \qquad (6a)$$

for axial channeling $$Y_P = n \cdot L_C \cdot \iint \frac{d\sigma_{CH}(Z, E_P, E_\gamma)}{dE_P d\Omega} \Delta\Omega dE_\gamma dE_P \, , \qquad (6b)$$

where n is the number of atoms per volume unit of W convertor, L is the convertor thickness,

$$\Delta\Omega = \left(\int \frac{dW}{d\hbar\omega dL} d\hbar\omega \right) / \left(\int \frac{dW}{d\Omega d\hbar\omega dL} d\hbar\omega \right) = \left(Y_{CR} \right) / \left(L \int \frac{dW}{d\Omega d\hbar\omega dL} d\hbar\omega \right) \approx 1.26 \cdot 10^{-5}$$

– average radiation angle, Y_{CR} – the total yield of CR from 200 MeV electron in W [18].

The results of simulation of photoproduction of positrons in thin W amorphous converter by CR and B are presented in Tab. 2. In the frame of the Scheme No3 for positron photoproduction, the increasing of the initial electron beam energy in 4 times (from 200 MeV to 800 MeV) leads to increasing of positron yield approximately by 250 (!) times and spreading of the positron spectrum by 9 times (according to FWHM). Further increasing of the initial electron beam energy up to 1.6 GeV leads to increasing of positron yield by 2.5 times and spreading of the positron spectrum by 2 times. At the increase of the initial electron beam energy from 200 MeV to 1600 MeV the maximum position of the function $\sigma(E_P)$ (5) shifts from 1 MeV to 3 MeV. Thus, in the considered Scheme No.3 the emitted positrons predominantly possess low kinetic energy.

Table 2: The positron spectra features.

Radiation type (W radiator thickness L=10 μm)	The position of the maximum of function $\sigma(E_P)$ (5), MeV	The height of the maximum of function $\sigma(E_P)$ (5), barn/MeV	FWHM of $\sigma(E_P)$ (5), MeV	Total yield of e^+/e^- in a 0.1 mm W converter, Y_P (6)	Positrons yield within energy range 1÷3 MeV
200 MeV (110)	1.03	$1.30\ 10^{-3}$	0.91	$1.0\ 10^{-9}$	$9.6\ 10^{-10}$
800 MeV (110)	2.26	0.043	8.31	$2.4\ 10^{-7}$	$5.0\ 10^{-8}$
1600 MeV (110)	3.24	0.045	17.34	$6.2\ 10^{-7}$	$5.2\ 10^{-8}$
200 MeV <100>	1.72	0.101	4.46	$4.7\ 10^{-7}$	$1.6\ 10^{-7}$
200 MeV B	1.88	0.014	7.99	$1.6\ 10^{-7}$	$1.5\ 10^{-8}$

5 POSITRON STOPPING IN CONVERTOR

The converter thickness selection is determined by two counter conditions. The converter thickness growth leads to the increase of the probability of the electron-positron pair photoproduction. But, production of electron-positron pairs occurs in the converter bulk. Thus, before leaving the converter, the positrons release their kinetic energy. If the converter is thick enough, the positrons lose energy down to zero, and successfully annihilate. These two mechanisms are defined by two parameters: λ - the mean free path of a photon before convertion into electron-positron pair and mean free path of a positron in matter until its

annihilation. The first parameter can be calculated using total cross-section of electron-positron pair production Eq.(2):

$$\lambda(Z, E_\gamma) = \frac{1}{n(Z) \cdot \sigma_{tot}(Z, E_\gamma)}, \tag{7}$$

For the second parameter determination, the simulation of the positron passage through the converter material is carried out. The results of the CASINO code [23] simulation for the average length of total energy loss of the electrons are shown in Fig. 10.

Moreover, the passage of positrons through the converter leads to the positron energy loss, thus, the positron spectrum change should be taken into account.

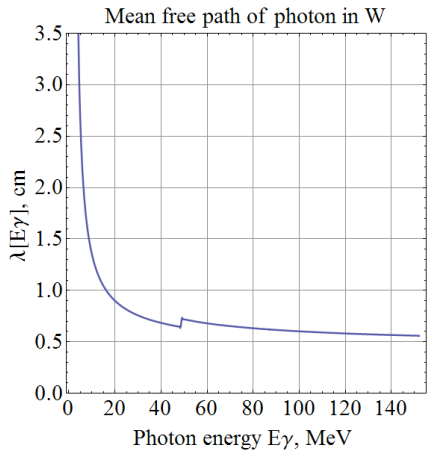

Figure 9: The mean free path of photon in W (8).

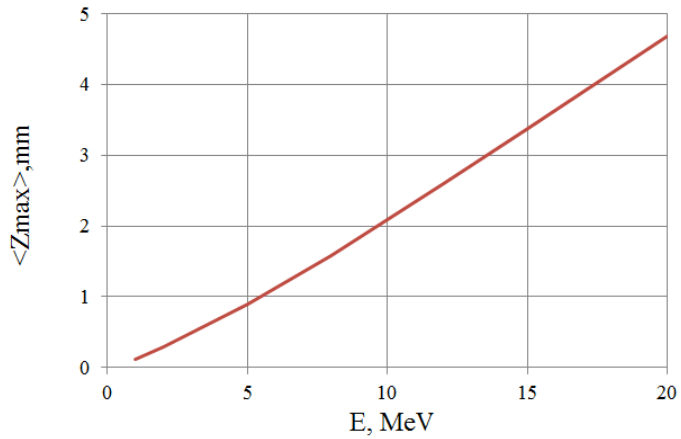

Figure 10: Average thickness of penetration of electron into W. The simulations done by CASINO [23].

6 CONCLUSIONS

The intensity spectra of the radiation from (110) planar channeled 200, 800 and 1600 MeV electrons and from <100> axially channeled 200 MeV electrons in W are obtained by means of computer modelling. Maxima of the radiation spectra correspond to the photon energies 1.5 MeV, 15 MeV, 42 MeV and 5 MeV, respectively.

The energy spectra of positrons generated in a thin amorphous W converter by radiation from 200, 800 and 1600 MeV electrons at (110) planar channeling and from 200 MeV electrons at <100> axial channeling in W radiator. The results are shown in Table 2.

For the hybrid positron source using initial 200 MeV electron beam and thin (0.1 mm) amorphous converter, the estimated yield of positrons in the energy range $1 \div 3$ MeV is about 10^{-6} e^+/e^- (almost 100% of the total yield) for (110) planar channeling and $1.5\ 10^{-5}$ e^+/e^- (less than 10% of the total yield) in the case of bremsstrahlung.

According to Table 2 and SPARC_LAB electron parameters [24] (bunch charge 1.1 nC, repetition rate $1 \div 10$ Hz) the utilization of CR by 200 MeV electrons in a 10 μm W (110) radiator and 0.1 mm convertor gives the positron yield of about $10 \div 10^2$ e^+ per second. In the case of CR at <100> axial channeled with all other parameters unchanged the positron yield is about $10^3 \div 10^4$ e^+ per second.

The yield of positrons can be increased if applied to both radiator and converter of larger thicknesses that reveals the necessity to take into account the features of the projectile dechanneling and the crystal collimation.

7 ACKNOWLEDGEMENTS

The work was supported by National Research Tomsk Polytechnic University (Grant "Mobility for young researchers"), LNF Frascati, President Grant No MK-237.2013.2, RFBC frant No 12-02-01314-a and partially by Government Grant "Nauka" No 1.676.2014/K. One of the authors (SD) would like to acknowledge the support by the Ministry of Education and Science of Russian Federation in the frames of Competitiveness Growth Program of NRNU MEPhI, Agreement 02.A03.21.0005.

8 REFERENCES

(1) I.N. Meshkov, Phys. Part. Nucl. **28(2)**, 198, (1997); doi: 10.1134/1.953037.
(2) I.N. Meshkov, in: Proc. International Symposium on Hadronic Atoms and Positronium in the Standard Model (26–31 May 1998), **1**, 176, (Russia, Dubna, 1998).
(3) I.N. Meshkov, A.N. Skrinsky, Nucl. Instr. and Meth. **A 391**, 205, (1997).
(4) J.P. Merrison, H. Bluhme, N. Hertel, H. Knudsen, and E. Uggerhøj: Proceedings of the XX International Conference on the Physics of Electronic and Atomic Collisions (1997), 210, (Vienna, Austria, 1997)
(5) K. Yoshida et al., Phys. Rev. Lett. **80 (7)**, 1437, (1998).
(6) V.N. Baier et al., Nucl. Instr. and Meth. **B 145** (1,2), 221, (1998).
(7) B.N. Kalinin et al., Nucl. Instr. and Meth. **B 145** (1,2), 209, (1998).
(8) M. Inoue et al., Nucl. Instr. and Meth. **B 173** (1–2), 104, (2001).
(9) R. Chehab et al. Physics Letters **B 525**, 41, (2002).
(10) V.A. Dolgikh, Yu.P. Kunashenko, Yu.L. Pivovarov Nucl. Instr. Meth. **B 201**, 253, (2003).
(11) X. Artru, R. Chehab, M. Chevallier, V.M. Strakhovenko, A. Variola, A. Vivoli Nucl. Instr. Meth. **B 266**, 3868, (2008).
(12) G.Alexander, J.Barley, Y.Batygin, et al. Phys. Rev. Lett. **V.100** ,P.210801, (2008).
(13) Backe H., Kunz P., Laulh W. et al. Nucl. Instr. Meth. **B 266**, P. 3835, (2008).
(14) V.N. Baier, V.M. Katkov, V.M. Strakhovenko, Electromagnetic Processes at High Energy in Oriented Single Crystals, World Scientific, Singapore, (1998).
(15) S.B. Dabagov, N.K. Zhevago, Riv. Nuovo Cimento 31, P. 491 (2008).

(16) E.G. Vyatkin, Yu.L. Pivovarov, S.A. Vorobiev, Nucl. Phys. **B 284**, 509, (1987).
(17) O.V. Bogdanov, E.I. Fiks, K.B. Korotchenko, Yu.L. Pivovarov, T.A.Tukhfatullin J. of Phys.: Conf. Ser. **236**, 1, (2010); doi:10.1088/1742-6596/236/1/012029.
(18) S.V. Abdrashitov, O.V. Bogdanov, S.B. Dabagov, Yu.L. Pivovarov, T.A. Tukhfatullin Nucl. Instr. Meth. **B 309C**, 59, (2013); DOI 10.1016/j.nimb.2013.02. 020.
(19) H.W. Koch, and J.W. Motz, Rev. Mod. Phys. **31**, 920, (1959).
(20) A.I. Akhiezer, V.B. Berestetsky, Quantum Electrodynamics, Nauka Publishing House, Moscow, (1981).
(21) A.N. Kalinovskii; N.V. Mokhov; Yu. P. Nikitin, Passage of high-energy particles through matter, American Institute of Physics, New York, (1989).
(22) W. Heitler, The Quantum Theory of Radiation, Oxford University Press, London, (1957).
(23) D. Drouin, A. R. Couture, D. Joly, X. Tastet, V. Aimez and R. Gauvin Scanning **29 (3)**, 92, (2007).
(24) SPARC Parameters. URL: http://www.lnf.infn.it/acceleratori/sparc/